Violation of Bell's Inequality with Continuous Variables and Fractional Fourier Transforms

S. P. Walborn,* D. S. Tasca, M. P. Almeida, and P. H. Souto Ribeiro
Instituto de Física, Universidade Federal do Rio de Janeiro,
Caixa Postal 68528, Rio de Janeiro, RJ 21941-972, Brazil

P. Pellat-Finet
Groupe d'Optique Théorique et Appliquée, Université de Bretagne Sud, B. P. 92116, Lorient cedex, France and
Département d'Optique, UMR CNRS 6082, École Nationale Supérieure des Télécommunications de Bretagne, France

C. H. Monken
Departamento de Física, Universidade Federal de Minas Gerais,
Caixa Postal 702, Belo Horizonte, MG 30123-970, Brazil
(Dated: December 2, 2024)

As originally formulated, Bell inequalities are expressed in terms of two-dimensional dichotomic observables. For this reason, systems like spin 1/2 particles and photon polarization were immediately identified as suitable for experimental realization of Bell inequalities violations. Continuous variable systems can also be used to display quantum nonlocality, but discretization is always necessary in order to implement a test of Bell's inequality. Here we show that violation of a Bell inequality is possible with the the transverse momentum of photons produced by parametric down-conversion when one discretizes the system and uses fractional fourier transforms for implementing rotations in the phase space. We present a multimode quantum calculation of the coincidence count rates, which predicts the violation of the CHSH inequality for realistic experimental parameters. We also provide a more pedagogical and intuitive explanation of these results based on Klyshko's advanced wave picture and geometric optics.

I. INTRODUCTION

The discussion about non-local correlations between properties of two separated particles began with the famous "EPR" paper [1]. Einstein, Podolsky and Rosen used the position and momentum of two correlated particles to construct a paradox between the quantum theory and intuitive concepts like locality and reality of physical properties. It may be somewhat surprising that thirty years passed before anyone returned to the problem and proposed a method to test quantum mechanics against local realistic theories. It was in 1965, that John Bell developed such a test [2]. However, instead of position and momentum of two particles, his derivation was inspired by David Bohm's version of the EPR paradox [3], which is based on a correlation between spin-1/2 particles. In addition to the fundamental aspect concerning the nonlocality and completeness of quantum mechanics, the violation of a Bell inequality has become a useful way to prove the non-classical character of correlations between the properties of two particles. Therefore, as the inequality does not apply in principle to continuous variables, a number of systems which present correlations between continuous observables could not be checked with this kind of test. In fact, John Bell [4] argued that position and momentum of particles could not be used in Bell inequalities because a typical EPR state can be described by a positive Wigner function and therefore an obvious hidden variable model.

On the one hand, despite these arguments against the use of continuous variables in this context, it has been demonstrated theoretically [5, 6, 7, 8] and experimentally [9], that continuous variables can indeed be used to violate Bell's inequalities. On the other hand, since these variables are required to be dichotomic, one has to discretize the measurements of the continuous variable, in order to apply a Bell inequality. Banaszek et al. [6] demonstrate that a Bell inequality can be violated for a state with positive Wigner functions. The observable related to the direct measurement of the Wigner function is the displaced parity operator, which is a dichotomic observable. It was pointed out by Kusmich et al.[9] that the state of a given system is not enough to determine whether it is suitable or not for this kind of experiment. One must also take into account, the observables measured.

In this paper, we present a theoretical treatment which enables us to predict the coincidence count rate and consequently predict the correlation functions for a Bell inequality experiment using the transverse momentum of a pair of photons. We consider the experiment reported in reference [10], which It consists of performing correlated measurements of the generalized transverse momentum. of photons. Particular cases of this physical property are the position and ordinary momentum. The generalization is obtained with the optical implementation of the Fractional Fourier Transform (FRFT) [11, 12, 13, 14] of the field at the source. For this reason we have chosen

*swalborn@if.ufrj.br

to refer to this generalized momentum as the fractional momentum of the photon. In practice, a projection onto an arbitrary fractional momentum can always be implemented with propagation through lenses.

This paper is organized as follows. First we introduce the Bell-Clauser-Horne-Shimony-Holt inequality and discuss the discretization of the transverse momentum and the measurements necessary to implement an experimental test. In section III, we calculate the coincidence count rates using a multimode quantum theory. This theoretical approach was developed by Monken et al. [15] and used to described a number of experiments exploring the transverse spatial correlations between twin photons[16, 17, 18, 19, 20, 21, 22, 23]. The results show that the Bell inequality can be nearly optimally violated. In section IV, we present a simple and intuitive method for calculating the coincidence count rates based on Klyshko's advanced wave picture and ray optics. In this case the coincidence count rates are proportional to portions of a phase space distribution, which are easily calculated using simple geometry. In both cases, our theoretical results are in agreement with the experimental results presented in reference [10].

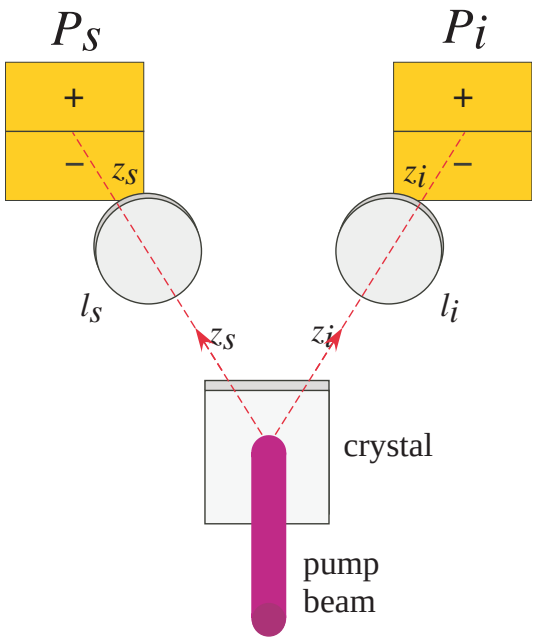

FIG. 1: Schematic of the proposed experiment.

II. THE BELL-CHSH INEQUALITY

The majority of experiments testing quantum nonlocality rely on violation of the Bell-Clauser-Horne-Shimony-Holt (CHSH) inequality [24, 25], which, for any classical hidden variable theory, predicts $-2 \leq \mathcal{S} \leq 2$, where

$$\mathcal{S} = E(\alpha_1, \alpha_2) + E(\alpha_1, \alpha_4) + E(\alpha_3, \alpha_2) - E(\alpha_3, \alpha_4), \quad (1)$$

and

$$E(\alpha, \beta) = \frac{C(\alpha, \beta) + C(\bar{\alpha}, \bar{\beta}) - C(\bar{\alpha}, \beta) - C(\alpha, \bar{\beta})}{C(\alpha, \bar{\beta}) + C(\bar{\alpha}, \bar{\beta}) + C(\bar{\alpha}, \beta) + C(\alpha, \bar{\beta})} \quad (2)$$

is the correlation function and $C(\alpha, \beta)$ is the number of coincidence counts for analyzer settings α and β. The Bell-CHSH inequality in this form is applicable to dichotomic observables, so that a measurement in the α basis gives either result α or $\bar{\alpha}$ with respective probabilities $P(\alpha)$ and $P(\bar{\alpha})$, and $P(\alpha) + P(\bar{\alpha}) = 1$. It is well known that, in contrast to classical theories, for certain measurements on appropriate two-level systems quantum mechanics predicts values up to $|\mathcal{S}| = 2\sqrt{2}$, known as Cirel'son's bound [26].

Consider the experiment outlined in Fig. 1, in which a pair of photons created by spontaneous parametric down-conversion (SPDC) pass through separate optical lens systems and are detected at detection planes P_s and P_i. Here s and i refer to the "signal" and "idler" photons. The lens systems will be used to implement the fractional Fourier transform of the signal and idler fields, each transformation being characterized by a variable order parameter ϕ_s and ϕ_i, respectively. The FRFT will be discussed in more detail below, for now it suffices to mention that the parameters ϕ_s and ϕ_i will play the role of analyzer settings for the CHSH inequality.

Here we will be working with the transverse spatial degrees of freedom of the photon pairs, which are continuous degrees of freedom. Thus, in order to use the CHSH inequality in the form (1), it is necessary to dichotomize the transverse spatial variables [6, 7, 8, 27]. We will do this by simply dividing the detection region into two regions, an upper "+" region and a lower "−" region. Then, for FRFT orders ϕ_s and ϕ_i, $C(\phi_s^+, \phi_i^+)$ denotes the number of events in which both the signal and idler photons fall in the "+" region. Any coincidence event thus falls in one of the four possibilities: $C(\phi_s^+, \phi_i^+)$, $C(\phi_s^+, \phi_i^-)$, $C(\phi_s^-, \phi_i^+)$, or $C(\phi_s^-, \phi_i^-)$.

The rest of this paper will be dedicated to calculation of the coincidence count rates $C(\phi_s, \phi_i)$. In section III we use the usual multimode quantum optics formalism, and in section IV we adopt a more intuitive and pedagogical approach using ray optics and Klyshko's advanced wave picture [28]. In both cases that it is possible to violate the Bell-CHSH inequality (1) with realistic experimental parameters.

III. MULTIMODE QUANTUM THEORY

Let us assume that a ϕ_s-order FRFT is performed on the signal field and a ϕ_i-order FRFT on the idler field. The coincidence count rate for a point detector placed at position $\boldsymbol{\rho}_s$ in the signal beam and a point detector placed at position $\boldsymbol{\rho}_i$ in the idler beam is proportional to the two-photon detection probability $P(\boldsymbol{\rho}_s, \phi_s; \boldsymbol{\rho}_i, \phi_i) =$

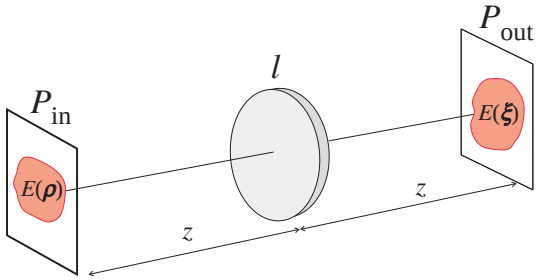

FIG. 2: A simple optical system which implements the FRFT. Here F is the focal length of the lens, and $z = 2l\sin^2(\phi/2)$.

$|\Psi(\boldsymbol{\rho}_s, \phi_s; \boldsymbol{\rho}_i, \phi_i)|^2$, where

$$\Psi(\boldsymbol{\rho}_s, \phi_s; \boldsymbol{\rho}_i, \phi_i) = \langle \text{vac}| \, \mathsf{E}_{\phi_s}(\boldsymbol{\rho}_s)\mathsf{E}_{\phi_i}(\boldsymbol{\rho}_i) \, |\psi\rangle \,, \quad (3)$$

is the two-photon detection amplitude. Here $|\psi\rangle$ is the two-photon state at the source and $\mathsf{E}(\boldsymbol{\rho}, \phi)$ is the field operator which detects a photon at transverse position $\boldsymbol{\rho} = (x, y)$. The field operator for the optical FRFT will be calculated in section III B.

The coincidence count rate for a signal and idler detectors with detection apertures $\mathcal{A}_s(\boldsymbol{\rho}_s)$ and $\mathcal{A}_i(\boldsymbol{\rho}_i)$ is obtained by integrating the two-point detection probability $P(\boldsymbol{\rho}_s, \phi_s; \boldsymbol{\rho}_i, \phi_i)$ over the detection apertures:

$$C(\phi_s, \phi_i) = \iint d\boldsymbol{\rho}_s d\boldsymbol{\rho}_i P(\boldsymbol{\rho}_s, \phi_s; \boldsymbol{\rho}_i, \phi_i)\mathcal{A}_s(\boldsymbol{\rho}_s)\mathcal{A}_i(\boldsymbol{\rho}_i). \quad (4)$$

There has been much work dedicated to describing the two-photon state produced by SPDC. In the thin crystal and monochromatic approximations, the post-selected two-photon state $|\psi\rangle$ at the crystal face is [15, 19]

$$|\psi\rangle = \iint d\mathbf{q}_s d\mathbf{q}_i v(\mathbf{q}_s + \mathbf{q}_i)\gamma(\mathbf{q}_s - \mathbf{q}_i) \, |\mathbf{q}_s\rangle \, |\mathbf{q}_i\rangle \,, \quad (5)$$

where $v(\mathbf{q})$ is the angular spectrum of the pump beam at the crystal face, $\gamma(\mathbf{q})$ is the phase matching function of the non-linear crystal, and $\mathbf{q}_s$ and $\mathbf{q}_i$ are the transverse components of the wave vector. For simplicity, we will assume that the down-converted photons are degenerate, that is $k_s = k_i = K/2$, where K is the magnitude of the pump beam wave vector. In this case, $\gamma(\mathbf{q})$ is given by the normalized function [21]

$$\gamma(\mathbf{q}) = \sqrt{\frac{2L}{\pi^2 K}} \text{sinc}\left(\frac{L}{4K}|\mathbf{q}_s - \mathbf{q}_i|^2\right). \quad (6)$$

A. Optical Fractional Fourier Transform

Let us briefly review some important aspects of the FRFT and it's optical implementation. Since it's first appearance in 1929 [29], the FRFT has found widespread use in quantum mechanics [30, 31, 32] as well as signal processing and optics [33]. The FRFT of order ϕ of an input optical field $E(\boldsymbol{\rho})$ can be defined as [14]

$$\mathcal{F}_\phi[E](\boldsymbol{\xi}) \propto \exp\left(-\frac{ik\xi^2\cot\phi}{2f}\right) \times \iint \exp\left(-\frac{ik\rho^2\cot\phi}{2f}\right)\exp\left(\frac{ik\boldsymbol{\rho}\cdot\boldsymbol{\xi}}{f\sin\phi}\right)E(\boldsymbol{\rho})d\boldsymbol{\rho}, \quad (7)$$

where $\boldsymbol{\rho}$ and $\boldsymbol{\xi}$ are two-dimensional variables, k is the magnitude of the wave vector, and f is type of a scaled focal length. We note that $\phi = \pi/2$ corresponds to the usual Fourier transform, while $\phi = \pi$ corresponds to the usual $2f$ imaging system. Just as the Fourier transform appears naturally in the context of Franhauffer diffraction, it has been shown that the FRFT appears in the Fresnel diffraction regime [14]. It has also been shown that one can implement a FRFT using lenses [13, 34]. For example, consider the symetrical optical system shown in Fig. 2. Here l is the focal length of the lens and z is the propagation distance before and after the lens. Using $z = 2l\sin^2(\phi/2)$ and $f = l\sin\phi$, it has been shown that this optical system implements the FRFT operation given by Eq. (7).

B. Field Operator for FRFT system

Using usual methods in Fourier optics, the paraxial field operator for a single-lens fractional Fourier transform (FRFT) system as shown in Fig. 2 is given by

$$\mathsf{E}_\phi(\boldsymbol{\rho}) \propto \iint d\mathbf{q}d\mathbf{q}' \exp\left(-i\frac{(q^2 + q'^2)z}{2k}\right) \times \exp\left(i\frac{l}{2k}|\mathbf{q} - \mathbf{q}'|^2\right)e^{i\mathbf{q}\cdot\boldsymbol{\rho}}\mathsf{a}(\mathbf{q}'), \quad (8)$$

The operator $\mathsf{E}_\phi(\boldsymbol{\rho})$ destroys a photon at detector transverse position $\boldsymbol{\rho} = (x, y)$ at the output plane. We note that the operator $\mathsf{a}(\mathbf{q}')$ is expressed in terms of the input plane q-vector coordinates. Using $z = 2l\sin^2(\phi/2)$, $\mathsf{E}_\phi(\boldsymbol{\rho})$ can be put in the form

$$\mathsf{E}_\phi(\boldsymbol{\rho}) \propto \exp\left(-i\frac{k\tan\phi}{2f}\rho^2\right) \times \int d\mathbf{q}\exp\left(-i\frac{f\tan\phi}{2k}q^2\right)\exp\left(i\frac{\boldsymbol{\rho}\cdot\mathbf{q}}{\cos\phi}\right)\mathsf{a}(\mathbf{q}), \quad (9)$$

where $f = l\sin\phi$ is the scaled focal length of the lens with focal length l [13], which allows for identification with the FRFT given in Eq. ((7)). One can see that Eq. (9) is similar, but not identical to the FRFT given by Eq. (7). In fact, the tangent and cosine functions appear in (9) instead of cotangent and sine functions due to the fact that the FRFT is now being performed in q-space. For

the special case of the usual Fourier transform ($\phi = \pi/2$), Eq. (8) gives

$$\mathsf{E}_{\frac{\pi}{2}}(\boldsymbol{\rho}) \propto \mathsf{a}\left(\frac{k}{f}\boldsymbol{\rho}\right). \tag{10}$$

We will now calculate the detection amplitude for the correlation functions necessary in Eq. (2). For simplicity, we will assume that $f_s = f_i = f$.

C. ϕ_s–$\frac{\pi}{2}$ Correlation

The detection amplitude $\Psi_{\phi_s,\frac{\pi}{2}}(\boldsymbol{\rho}_s,\boldsymbol{\rho}_i)$ associated with a ϕ_s FRFT on the signal photon and a $\pi/2$ FRFT on the idler photon is

$$\begin{aligned}\Psi_{\phi_s,\frac{\pi}{2}}(\boldsymbol{\rho}_s,\boldsymbol{\rho}_i) \propto &\exp\left(-i\frac{k\tan\phi_s}{2f}\rho_s^2\right)\times\\ &\int d\mathbf{q}_s \exp i\left(\frac{\boldsymbol{\rho}_s\cdot\mathbf{q}_s}{\cos\phi_s} - \frac{f\tan\phi_s q_s^2}{2k}\right)\\ &v(\mathbf{q}_s + k\boldsymbol{\rho}_i/f)\gamma(\mathbf{q}_s - k\boldsymbol{\rho}_i/f).\end{aligned} \tag{11}$$

Let us assume that the angular spectrum $v(\mathbf{q})$ of the pump beam is much narrower than the phase matching function $\gamma(\mathbf{q})$. Then, one can see immediately from Eq. (11) that $\Psi_{\phi_s,\frac{\pi}{2}}(\boldsymbol{\rho}_s,\boldsymbol{\rho}_i)$ is a ϕ_s-order FRFT of the function $v(\mathbf{q}_s + k\boldsymbol{\rho}_i/f)$. Defining $\boldsymbol{\zeta} = \mathbf{q}_s + k\boldsymbol{\rho}_i/f$, Eq. (11) can be put in the form

$$\begin{aligned}\Psi_{\phi_s,\frac{\pi}{2}}(\boldsymbol{\rho}_s,\boldsymbol{\rho}_i) \propto &\exp\left[-i\frac{k\tan\phi_s}{2f}(\rho_s^2+\rho_i^2) - i\frac{k}{f}\frac{\boldsymbol{\rho}_s\cdot\boldsymbol{\rho}_i}{\cos\phi_s}\right]\times\\ &\int d\boldsymbol{\zeta}\exp\left[i\boldsymbol{\zeta}\cdot\left(\frac{\boldsymbol{\rho}_s}{\cos\phi_s} + \tan\phi_s\boldsymbol{\rho}_i\right)\right]\times\\ &\exp\left(-i\frac{f\tan\phi_s\zeta^2}{2k}\right)v(\boldsymbol{\zeta}),\end{aligned} \tag{12}$$

which is a shifted fractional Fourier transform. The shift is given by the factor $-\sin\phi_s\boldsymbol{\rho}_i$.

Let us suppose that the angular spectrum of the pump beam is a Gaussian function, given by

$$v(\mathbf{q}) = \exp(-q^2/2\sigma^2). \tag{13}$$

Then, performing the shifted fractional Fourier transform in Eq. (12), the detection amplitude is

$$\begin{aligned}\Psi_{\phi_s,\frac{\pi}{2}}(\boldsymbol{\rho}_s,\boldsymbol{\rho}_i) \propto &\exp\left[-i\frac{k\tan\phi_s}{2f}(\rho_s^2+\rho_i^2) - i\frac{k}{f}\frac{\boldsymbol{\rho}_s\cdot\boldsymbol{\rho}_i}{\cos\phi_s}\right]\times\\ &\exp\left[-\frac{\sigma^2}{2}\frac{(\boldsymbol{\rho}_s+\sin\phi_s\boldsymbol{\rho}_i)^2}{\cos\phi_s + i\sigma^2 f\sin\phi_s/k}\right],\end{aligned} \tag{14}$$

while the detection probability is

$$P_{\phi_s,\frac{\pi}{2}}(\boldsymbol{\rho}_s,\boldsymbol{\rho}_i) \propto \exp\left[-\sigma^2\frac{(\boldsymbol{\rho}_s+\sin\phi_s\boldsymbol{\rho_i})^2}{\cos^2\phi_s + 4\sigma^4 f^2\sin^2\phi_s/K^2}\right]. \tag{15}$$

We have written Eq. ((**??**)) in terms of the pump beam wave number $K = 2k$. The coincidence count rate $C(\phi_s, \frac{\pi}{2})$ for detectors equipped with half plane apertures is given by integrating Eq. (15) over the areas defined by the apertures, as shown in Eq. (4).

D. ϕ_s–π Correlation

The detection amplitude $\Psi_{\phi_s,\pi}(\boldsymbol{\rho}_s,\boldsymbol{\rho}_i)$ for a ϕ_s FRFT on the signal photon and a π FRFT on the idler photon is

$$\begin{aligned}\Psi_{\phi_s,\pi}(\boldsymbol{\rho}_s,\boldsymbol{\rho}_i) \propto &\exp\left(-i\frac{k\tan\phi_s}{2f}\rho_s^2\right)\times\\ &\int d\mathbf{q}_s\exp\left(i\frac{\boldsymbol{\rho}_s\cdot\mathbf{q}_s}{\cos\phi_s} - i\frac{f\tan\phi_s q_s^2}{2k}\right)\\ &\int d\mathbf{q}_i\exp(-i\boldsymbol{\rho}_i\cdot\mathbf{q}_i)\\ &v(\mathbf{q}_s+\mathbf{q}_i)\gamma(\mathbf{q}_s-\mathbf{q}_i).\end{aligned} \tag{16}$$

Changing coordinates to

$$\begin{aligned}\mathbf{Q} &= \mathbf{q}_s + \mathbf{q}_i,\\ \mathbf{P} &= \mathbf{q}_s - \mathbf{q}_i,\\ \mathbf{R} &= \frac{1}{2}\left(\frac{\boldsymbol{\rho}_s}{\cos\phi_s} - \boldsymbol{\rho}_i\right),\\ \mathbf{S} &= \frac{1}{2}\left(\frac{\boldsymbol{\rho}_s}{\cos\phi_s} + \boldsymbol{\rho}_i\right),\end{aligned} \tag{17}$$

the detection amplitude becomes

$$\begin{aligned}\Psi_{\phi_s,\pi}(\boldsymbol{\rho}_s,\boldsymbol{\rho}_i) \propto &\exp\left(-i\frac{k\tan\phi_s}{2f}\rho_s^2\right)\times\\ &\int d\mathbf{Q}\exp\left(i\mathbf{R}\cdot\mathbf{Q} - i\frac{f\tan\phi_s Q^2}{8k}\right)v(\mathbf{Q})\\ &\int d\mathbf{P}\exp\left[i\mathbf{P}\cdot\left(\mathbf{S} - \frac{f\tan\phi_s}{4k}\mathbf{Q}\right)\right]\times\\ &\exp\left(-i\frac{f\tan\phi_s P^2}{8k}\right)\gamma(\mathbf{P}).\end{aligned} \tag{18}$$

The $d\mathbf{P}$ integration can be performed using the convolution theorem [35]. After integration, the detection amplitude is

$$\begin{aligned}\Psi_{\phi_s,\pi}(\boldsymbol{\rho}_s,\boldsymbol{\rho}_i) \propto &\exp\left(-i\frac{k\tan\phi_s}{2f}\rho_s^2\right)\times\\ &\int d\boldsymbol{\eta}\exp\left(i\frac{2k\cot\phi_s}{f}|\boldsymbol{\eta}-\mathbf{S}|^2\right)\Gamma(\boldsymbol{\eta})\\ &\int d\mathbf{Q}v(\mathbf{Q})\exp\left[i\mathbf{Q}\cdot(\mathbf{R}+\boldsymbol{\eta}-\mathbf{S})\right],\end{aligned} \tag{19}$$

where $\Gamma(\boldsymbol{\rho})$ is the Fourier transform of the phase matching function $\gamma(\mathbf{q})$.The $d\mathbf{Q}$ integral is simply the field profile of the pump beam at $z = 0$:

$$\mathcal{U}(\boldsymbol{\rho}) \propto \int d\mathbf{q}v(\mathbf{q})\exp(i\mathbf{q}\cdot\boldsymbol{\rho}). \tag{20}$$

The detection amplitude is then

$$\Psi_{\phi_s,\pi}(\boldsymbol{\rho}_s,\boldsymbol{\rho}_i) \propto \exp\left(-i\frac{k\tan\phi_s}{2f}\rho_s^2\right)\times \int d\boldsymbol{\eta}\exp\left(i\frac{2k\cot\phi_s}{f}|\boldsymbol{\eta}+\mathbf{S}|^2\right)\times \Gamma(\boldsymbol{\eta})\mathcal{U}(\mathbf{R}+\boldsymbol{\eta}-\mathbf{S}). \quad (21)$$

If the angular spectrum $v(\mathbf{q})$ of the pump beam is much narrower than the phase matching function $\gamma(\mathbf{q})$, as was assumed in section III C, then the reverse is true for the Fourier transforms of these functions. That is, $\Gamma(\boldsymbol{\rho})$ must be narrower than $\mathcal{U}(\boldsymbol{\rho})$. Then, approximating $\mathcal{U}(vectR+\boldsymbol{\eta}-\mathbf{S})\sim$ constant, and again using $k=K/2$, we have

$$\Psi_{\phi_s,\pi}(\boldsymbol{\rho}_s,\boldsymbol{\rho}_i) \propto \exp\left(i\frac{K\boldsymbol{\rho_i}\cdot\boldsymbol{\rho_s}}{2f\sin\phi_s}\right) \exp\left[-i\frac{K\cot\phi_s}{4f}\left(\rho_i^2+\rho_s^2\right)\right]\times \int d\boldsymbol{\eta}\exp\left(i\frac{K\cot\phi_s}{f}\eta^2\right)\Gamma(\boldsymbol{\eta})\times \exp\left[\frac{iK}{f}\boldsymbol{\eta}\cdot\left(\frac{\boldsymbol{\rho}_s}{\sin\phi_s}+\cot\phi_s\boldsymbol{\rho}_i\right)\right]. \quad (22)$$

The function $\Gamma(\boldsymbol{\eta})$ is the Fourier transform of the phase matching function $\gamma(\mathbf{q})$. In the degenerate case, $\Gamma(\boldsymbol{\eta})\propto 1-2\mathrm{Si}(K\eta^2/4L)/\pi$ [36], where Si(x) is the sine integral. It is reasonable to approximate $\Gamma(\boldsymbol{\eta})$ by a Gaussian function of the form

$$\Gamma(\boldsymbol{\eta}) = \exp(-\eta^2/2\delta^2). \quad (23)$$

Then, performing the $d\boldsymbol{\eta}$ integration, the detection probability is

$$P_{\phi_s,\pi}(\boldsymbol{\rho}_s,\boldsymbol{\rho}_i) \propto \exp\left[-\frac{\Delta^2(\boldsymbol{\rho}_s+\cos\phi_s\boldsymbol{\rho_i})^2}{\delta^2(\sin^2\phi_s+4\Delta^4\cos^2\phi_s)}\right], \quad (24)$$

where $\Delta=\delta^2K/f$ The detection probabilities for both the $\phi_i=\pi/2$ case (15) and the $\phi_i=\pi$ case (24) are shifted Gaussian functions. In both cases, the center of each function depends on the angle ϕ_s of the signal FRFT. To violate Bell's inequality in this context, it is necessary to choose different sets of angles ϕ_s and ϕ_i. For polarization-based Bell's inequality experiments, it is customary to use the polarizer angles 0° and 45° at one analyzer, and the intermediate angles 22.5° and 67.5° at the other. Here we have calculated the detection probabilites for FRFT orders $\pi/2$ and π, and it thus seems natural to choose the intermediate orders $\phi_s=\{\phi_2=5\pi/4,\phi_4=3\pi/4\}$ for the signal analyzer settings. We note that, using a single lens, it is possible to implement an optical FRFT up to order $\phi=\pi$. However, larger orders, such as $\phi=5\pi/4$ can be performed using two lenses, due to the additivity property of the FRFT [11, 12].

TABLE I: Type of correlation for correlation functions. The position dependence is shown up to a scaling factor.

ϕ_s	ϕ_i	position dependence	type of correlation
$3\pi/4$	$\pi/2$	$\boldsymbol{\rho}_s+\frac{\boldsymbol{\rho_i}}{\sqrt{2}}$	anti-correlation
$3\pi/4$	π	$\boldsymbol{\rho}_s-\frac{\boldsymbol{\rho_i}}{\sqrt{2}}$	correlation
$5\pi/4$	$\pi/2$	$\boldsymbol{\rho}_s-\frac{\boldsymbol{\rho_i}}{\sqrt{2}}$	correlation
$5\pi/4$	π	$\boldsymbol{\rho}_s-\frac{\boldsymbol{\rho_i}}{\sqrt{2}}$	correlation

Before we determine a numerical prediction for the violation of the CHSH inequality, let us analyze our results in a qualitative manner. In order to violate Bell's inequality, it is necessary that three of the correlation functions in the CHSH inequality (1) have the same sign, while the fourth must have the opposite sign. In other words, if three of the correlation functions show a *correlation*, the fourth must show an *anti-correlation*. When the coincidence detection probability depends on the sum of the detector positions, we observe an anti-correlation in the coincidence detections, and when the detection probability depends on the difference of the detector positions, a correlation is observed. In order to violate the CHSH inequality, it is thus necessary that three of the detection probabilities display the same type of correlation, while the other displays the opposite type. Table I shows the type of correlation which should be observed for the four correlation functions.

Through numerical integration, we can show the violation of inequality (1) using typical experimental parameters. Considering that the pump beam profile is a Gaussian with width $w=4$mm, the width of the angular spectrum is $\sigma=1/w=0.25\mathrm{mm}^{-1}$. The width of the function $\Gamma(\boldsymbol{\rho})$, measured for a 5mm long $LiIO_3$ crystal, using 10nm FWHM interference filters, is about 5μm [37]. Using $\delta=5\mu$m, $K=442\,$nm, $l=500\,$mm, and considering a total detection region of 12 mm, we obtain $E(3\pi/4,\pi/2)=0.61$, $E(3\pi/4,\pi)=0.61$, $E(5\pi/4,\pi/2)=0.73$, $E(5\pi/4,\pi)=0.73$, giving $\mathcal{S}=E(5\pi/4,\pi)+E(3\pi/4,\pi)+E(5\pi/4,\pi/2)-E(3\pi/4,\pi/2)=2.68$, a violation of the Bell-CHSH inequality.

IV. ADVANCED WAVE PICTURE AND RAY OPTICS

A. Advanced Wave Picture

Klyshko's advanced wave picture (AWP) [28] along with ray optics allows us to provide a simple and intuitive explanation of a Bell's inequality experiment based on optical FRFT's. The AWP is a useful method for calculating the coincidence count rate, in which we imagine that–say–the signal detector at plane P_s is a source emitting a field in the reverse direction back towards the crystal, while the crystal acts as a mirror, reflecting the

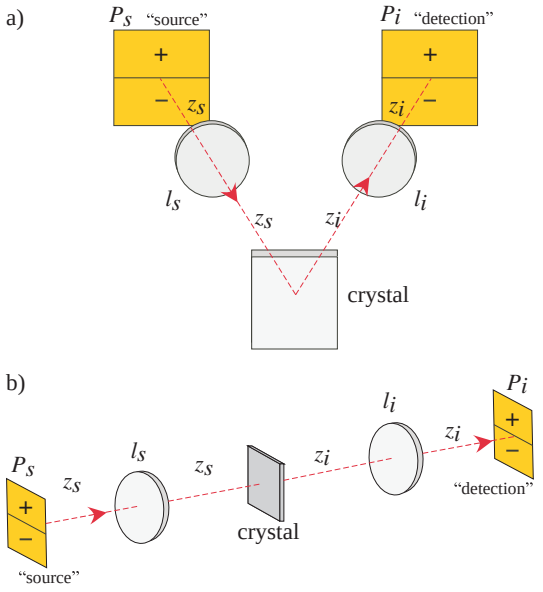

FIG. 3: a) Advanced wave picture applied to Bell's inequality experiment with fractional Fourier transforms. b) Topological equivalent of a), up to a reflection of the field.

field to detection plane P_i. The coincidence detection probability is determined by the probability to detect an "emitted" signal photon at the idler detector on plane P_i. In other words, the fourth-order correlation function is given by calculation of the second-order correlation function in the AWP representation. The AWP is known to produce results equivalent to those obtained with the standard methods [38].

FIG. 3 a) shows an illustration of the AWP applied to the experiment shown in FIG. 1, and FIG. 3 b) shows a topological equivalent. For simplicity, let us work in the context of ray optics, and suppose that an initial ray $\mathbf{r}_s = (\rho_s, \theta_s)$ is "emitted" from the signal detector. Here we consider only one spatial dimension. In ray optics, a paraxial ray $\mathbf{r} = (\rho, \theta)$ is represented by its transverse coordinate ρ and the angle θ it makes with the paraxial direction of propagation. The angle θ is related to the transverse momentum of the field by

$$\theta = \frac{q}{k}. \tag{25}$$

According to the AWP, after passing through the two FRFT systems and "reflecting" from the crystal face, the ray at the idler detector will be given by $\mathbf{r}_i = \mathsf{F}_{\phi_i}\mathsf{F}_{\phi_s}\mathbf{r}_s$, where F_ϕ is the operation which describes the optical FRFT system. We will now briefly discuss the FRFT operation in ray optics.

B. Fractional Fourier Transform in Ray Optics

Consider the symmetrical lens system shown in FIG. 2. Free propagation of an optical ray can be represented by the ABCD matrix [39]

$$\mathsf{S}_z = \begin{pmatrix} 1 & z \\ 0 & 1 \end{pmatrix}, \tag{26}$$

where z is the propagation distance. Passage through a thin lens is given by the matrix

$$\mathsf{L}_l = \begin{pmatrix} 1 & 0 \\ -1/l & 1 \end{pmatrix}, \tag{27}$$

where l is the focal length of the lens. Choosing $z = 2l\sin^2(\phi/2)$ and defining $f = l\sin\phi$ as a scaled focal length, the complete optical FRFT system is given by the matrix

$$\mathsf{F}_\phi = \mathsf{S}_z\mathsf{L}_l\mathsf{S}_z = \begin{pmatrix} \cos\phi & f\sin\phi \\ -\frac{1}{f}\sin\phi & \cos\phi \end{pmatrix}, \tag{28}$$

Matrix (28) represents a ϕ-order FRFT, and is recognized as a rotation matrix scaled by f. This scaling is necessary since ρ has dimension of length and θ is adimensional, and thus scaled focal length f acts on θ so that $f\theta$ has dimension of length. If the scaled focal lengths f of two FRFTs are equal, it is easy to see from the ray matrix in Eq. (28) that the FRFT is additive, that is $\mathsf{F}_{\phi_1}\mathsf{F}_{\phi_2} = \mathsf{F}_{\phi_1+\phi_2}$, such that the order of the combined optical FRFT is $\phi_1 + \phi_2$.

We can now define a fractional Fourier ray $\mathbf{r}_\phi$ as

$$\mathbf{r}_\phi = \mathsf{F}_\phi\mathbf{r} = \begin{pmatrix} \rho_\phi \\ \theta_\phi \end{pmatrix}, \tag{29}$$

The ordinary Fourier transform is obtained from F_ϕ by setting θ equal to $\pi/2$, and one can see that the fractional Fourier ray $\mathbf{r}_\phi$ can be expressed in terms of the original ray $\mathbf{r}$ and its Fourier ray $\mathbf{r}_F = \mathsf{F}_{\frac{\pi}{2}}\mathbf{r}$ as

$$\mathbf{r}_\phi = \cos(\phi)\mathbf{r} + \sin(\phi)\mathbf{r}_F. \tag{30}$$

Detection of the fractional Fourier ray gives us information about its transverse coordinate ρ_ϕ, which is a linear combination of ρ and θ:

$$\rho_\phi = \cos(\phi)\rho + \sin(\phi)f\theta. \tag{31}$$

Returning now to the AWP, using the additivity property of the FRFT, the idler ray is a fractional Fourier ray, given by the combined FRFT of the signal ray:

$$\mathbf{r}_i = \mathsf{F}_{\phi_i}\mathsf{F}_{\phi_s}\mathsf{r}_s = \mathsf{F}_{\phi_s+\phi_i}\mathbf{r}_s. \tag{32}$$

Eq. (32) illustrates the fact that the coincidence count rate depends on the sum of the individual FRFT orders.

Let us now consider an example which illustrates the use of the AWP to calculate the coincidence count rate. Suppose that $\phi_s = \phi_i = \pi/2$ so that $\phi_s + \phi_i = \pi$, which corresponds to an imaging system. In this case Eq. (30) gives $\mathbf{r}_i = -\mathbf{r}_s$. If the idler detector is a point detector,

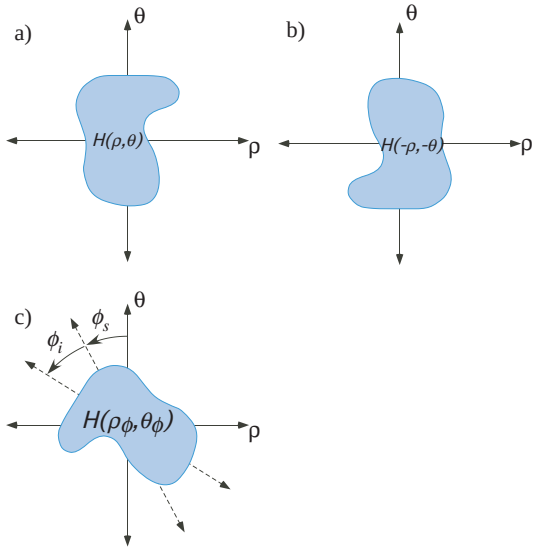

FIG. 4: a) Phase space distribution of an optical field. c) The ϕ-order FRFT corresponds to a rotation of angle ϕ in phase space.

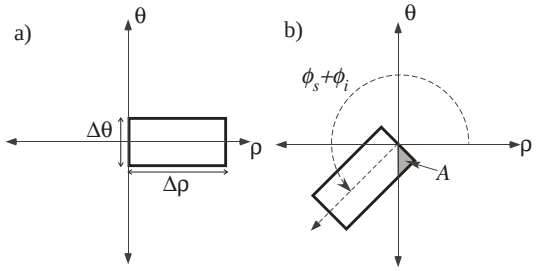

FIG. 5: a) AWP phase space distribution at the signal detector corresponding to a "+" measurement. For different measurement combinations, this distribution is rotated shown in b) for $\phi_s + \phi_i = 5\pi/4$. The detection probabilities can be calculated by determining the portion of the distribution that falls in the the positive ($\rho > 0$) or negative $\rho < 0$ half of phase space.

the AWP predicts that there will be coincidence counts only when it is placed at position $\rho_i = -\rho_s$. This type of correlation was indeed observed in [40]. Consider now that the spatial profile of the source (signal detector) is described by some function $s(\rho_s)$ and the detector (idler detector) is described by the function $d(\rho_i)$. When $\phi_s + \phi_i = \pi$, the image of the source is formed on the detection plane ($\mathbf{r}_i = -\mathbf{r}_s$), and thus the coincidence count rate is proportional to the product of the source function and detector function: $s(-\rho_i)d(\rho_i)$.

In general, the position component of the fractional Fourier ray (31) depends on the original θ component. So, in order to accurately calculate the coincidence detection probability for a general ϕ-order FRFT system, we must consider the complete position and angle distribution of the signal field.

C. Phase Space Representation

There is a convenient phase space representation of an optical field that can be constructed using the components of the ray vector [11, 13]. A ray $\mathbf{r} = (\rho, \theta)$ is represented by a point in phase space, while an optical field, which can be viewed as a bundle of rays, corresponds to a given phase space distribution. Suppose that the field "emitted" by the signal detector is given by the distribution $H(\rho, \theta)$, as shown in Fig. 4 a). Let us return now to our example in which $\phi_s + \phi_i = \pi$. In this case, the ray $\mathbf{r}_s = (\rho, \theta)$ is mapped to $\mathbf{r}_i = (-\rho, -\theta)$. As illustrated in Fig. 4 b), the phase space distribution of the field at the idler detector is equal to the original distribution, reflected about both the ρ and θ axes: $H_i(\rho_i, \theta_i) = H_s(-\rho_s, -\theta_s)$. In general, the effect of a FRFT of order ϕ is equivalent to a rotation of the phase space distribution by an angle ϕ in phase space [11, 13]:

$$H(\rho, \phi) \longrightarrow H(\rho_\phi, \theta_\phi) = H(\cos(\phi)\rho + \sin(\phi) f\theta, -\sin\phi\frac{\rho}{f} + \cos\phi\theta). \tag{33}$$

Thus, using the AWP, the phase space distribution of the idler field is given by phase space distribution of the signal field, rotated by an angle $\phi_i + \phi_s$, as shown in Fig. 4 c).

D. Bell's Inequality Violation

Let us consider an optical field with uniform position distribution $\Delta\rho$ and angle distribution $\Delta\theta$, which is represented in phase space by a rectangle. In the Bell inequality experiment we are considering here, the detection planes are divided into two halves (a "ϕ^+" region and a "ϕ^-" region). We will consider only one spatial dimension, so that the "+" region corresponds to $\rho > 0$ and the "−" region to $\rho < 0$. Let us assume that the initial field "emitted" by the signal detector is approximately described by the phase space distribution in FIG. 5 a), which corresponds to an upper "+" measurement, with only positive values of ρ. Upon propagation through the two FRFT systems, this phase space distribution will rotate an angle $\phi_s + \phi_i$, as illustrated in Fig. 5 b).

The detection probabilities can then be determined by considering different areas of the idler phase space distribution. For example, the coincidence count rate for detecting both signal and idler photons in the "+" detection region $C(\phi_s^+, \phi_i^+)$ can be calculated by determining the portion of the idler phase space distribution that lies in the positive-ρ half of phase space, while detecting the signal photon in the "+" region and the idler photon in the "−" region $C(\phi_s^+, \phi_i^-)$ corresponds to the negative-ρ half of phase space. For example, using Fig. 6 as a

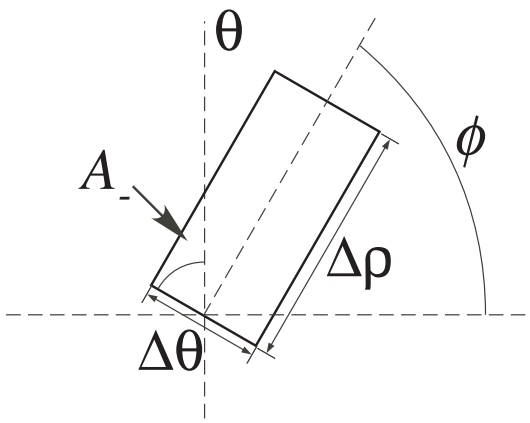

FIG. 6: The coincidence rate is proportional to the area above the positive and negative sides of the ρ axis.

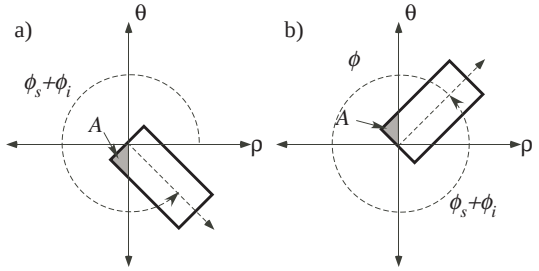

FIG. 7: Phase space rotations for different measurement combinations: a) $\phi_s + \phi_i = 7\pi/4$ and b) $\phi_s + \phi_i = 9\pi/4$. The detection probabilities can be calculated by determining the portion of the distribution that falls in the the positive ($\rho > 0$) or negative $\rho < 0$ half of phase space.

reference, provided that $\Delta\rho > \Delta\theta/2 \tan(\phi_s + \phi_i)$, then

$$C(\phi_s^+, \phi_i^-) = N\frac{A_-}{A_{\text{total}}} = N\frac{f\Delta\theta}{8\Delta\rho}\tan(\phi_s + \phi_i), \quad (34)$$

and

$$C(\phi_s^+, \phi_i^+) = N\frac{A_+}{A_{\text{total}}} = N\left(1 - \frac{A_-}{A_{\text{total}}}\right) = N\left(1 - \frac{f\Delta\theta}{8\Delta\rho}\tan(\phi_s + \phi_i)\right), \quad (35)$$

where A_+ (A_-) is the area of the phase space distribution on the positive (negative) side of the θ axis, $A_{\text{total}} = A_+ + A_-$ is the total area, and N is a proportionality constant. Here, as mentioned before, f is needed to maintain proper dimension [11]. Similarly, if we start with an initial phase space distribution corresponding to a "−" signal measurement (the same rectangle but reflected around the θ axis), we can determine $C(\phi_s^-, \phi_i^+)$ and $C(\phi_s^-, \phi_i^-)$. In this manner, it is possible to calculate a theoretical prediction for the value of the correlation functions $E(\phi_s, \phi_i)$ of the type defined in Eq. (2). Specifically, for the geometry shown in Fig. 6,

$$E(\phi_s, \phi_i) = 1 - 2\frac{f\Delta\theta}{8\Delta\rho}\tan(\phi_s + \phi_i). \quad (36)$$

As possible FRFT angles let us choose $\phi_s = \{\phi_1 = \pi, \phi_3 = \pi/2\}$ and $\phi_i = \{\phi_2 = 5\pi/4, \phi_4 = 3\pi/4\}$, so that $\phi_s + \phi_i$ is equal to either $5\pi/4$, $7\pi/4$ or $9\pi/4$. The phase space rotations corresponding to these FRFT's are shown in Fig.'s 5 b), 7a) and 7b). Then, provided that $\Delta\rho \geq f\Delta\theta/2$, it is straightforward to show that

$$\mathcal{S} = 4\left(1 - 2\frac{f\Delta\theta}{8\Delta\rho}\right). \quad (37)$$

We have $\mathcal{S} > 2$ whenever $f\Delta\theta/2 < \Delta\rho$, a violation of inequality (1). Given the size of the detection aperture and optical systems used in the experiment reported in [10], we calculate $\Delta\theta/2 \approx 0.42$ and $\Delta\rho \approx 6$mm, which gives a theoretical prediction of $\mathcal{S} = 2.6$, a violation of the CHSH inequality[41].

V. CONCLUSION

We have provided the theoretical basis behind a recent Bell's inequality experiment using transverse spatial degrees of freedom of photon pairs produced by parametric down-conversion [10]. The continuous spatial variables were dichotomized by dividing the detection regions into two halves. Using simple optical systems to implement the fractional Fourier transform of the signal and idler fields, it is possible to measure a "generalized momentum" of the down-converted photons. The coincidence detection probability was calculated using multimode quantum theory. The correlation functions and Bell parameter $\mathcal{S}$ were calculated numerically, and shown to violate the Bell-CHSH inequality. We also provided a more intuitive picture of this experiment based on ray optics and Klyshko's advanced wave picture. Both theoretical calculations show that it is possible to violate the Bell-CHSH inequality with transverse spatial degrees of freedom of photon pairs, supporting the experimental results obtained in Ref. [10].

Acknowledgments

We would like to thank E. Galvão, D. Jonathan and A. Z. Khoury for helpful conversations. Financial support was provided by Brazilian agencies CNPq, PRONEX, CAPES, FAPERJ, FUJB and the Millennium Institute for Quantum Information.

[1] A. Einstein, D. Podolsky, and N. Rosen, Phys. Rev. **47**, 777 (1935).
[2] J. Bell, Physics **1**, 195 (1965).
[3] D. Bohm, *Quantum Theory* (Prentice Hall, Englewood Cliffs, NJ, 1951).
[4] J. Bell, in *New Techniques and Ideas in Quantum Measurement Theory* (New York Academy of Sciences, 1986).
[5] K. Banaszek and K. Wódkiewicz, Phys. Rev. A **58**, 4345 (1998).
[6] K. Banaszek and K. Wodkiewicz, Phys. Rev. Lett. **82**, 2009 (1999).
[7] Z.-B. Chen, J.-W. Pan, G. Hou, and Y.-D. Zhang, Phys. Rev. Lett. **88**, 040406 (2002).
[8] G. Gour, F. C. Khanna, A. Mann, and M. Revzen, Phys. Lett. A **324**, 415 (2004).
[9] A. Kuzmich, I. A. Walmsley, and L. Mandel, Phys. Rev. Lett. **85**, 1349 (2000).
[10] D. S. Tasca, M. P. Almeida, S. P. Walborn, P. Pellat-Finet, C. H. Monken, and P. H. S. Ribeiro, quant-ph/0605061.
[11] D. Mendlovic and H. M. Ozaktas, J. Opt. Soc. Am. A **10**, 1875 (1993).
[12] H. M. Ozaktas and D. Mendlovic, J. Opt. Soc. Am. A **10**, 2522 (1993).
[13] A. W. Lohmann, Optics Comm. **115**, 437 (1995).
[14] P. Pellat-Finet, Opt. Lett. **19**, 1388 (1994).
[15] C. H. Monken, P. S. Ribeiro, and S. Pádua, Phys. Rev. A. **57**, 3123 (1998).
[16] E. Fonseca, C. Monken, and S. Pádua, Phys. Rev. Lett. **82**, 2868 (1999).
[17] W. A. T. Nogueira, S. P. Walborn, S. Pádua, and C. H. Monken, Phys. Rev. Lett. **86**, 4009 (2001).
[18] P. H. S. Ribeiro, D. P. Caetano, M. P. Almeia, J. A. Huguenin, B. C. dos Santos, and A. Z. Khoury, Phys. Rev. Lett. **87**, 133602 (2001).
[19] M. Atatüre, G. D. Giuseppe, M. D. Shaw, A. V. Sergienko, B. E. A. Saleh, and M. C. Teich, Phys. Rev. A **66**, 023822 (2002).
[20] D. P. Caetano and P. H. S. Ribeiro, Phys. Rev. A **68**, 043806 (2003).
[21] S. P. Walborn, A. N. de Oliveira, S. Pádua, and C. H. Monken, Phys. Rev. Lett **90**, 143601 (2003).
[22] S. P. Walborn, A. N. de Oliveira, R. S. Thebaldi, and C. H. Monken, Phys. Rev. A **69**, 023811 (2004).
[23] J. A. O. Huguenin, M. P. Almeia, P. H. S. Ribeiro, and A. Z. Khoury, Phys. Rev. A **71**, 043818 (2005).
[24] J. Clauser, M. Horne, A. Shimony, and R. Holt, Phys. Rev. Lett. **23**, 880 (1969).
[25] J. S. Bell, *Speakable and Unspeakable in Quantum Mechanics* (Cambridge University Presss, Cambridge, 1987).
[26] B. S. Cirel'son, Lett. Math. Phys. **4**, 93 (1980).
[27] K. Banaszek and K. Wodkiewicz, Phys. Rev. Lett. **76**, 4344 (1996).
[28] A. V. Belinski and D. N. Klyshko, JETP **78**, 259 (1994).
[29] N. Wiener, J. Math. Phys. MIT **8**, 70 (1929).
[30] V. Namias, J. Inst. Appl. Math. **25**, 241265 (1980).
[31] A. C. M. Bride and F. H. Kerr, IMA J. Appl. Math **39**, 159 (1987).
[32] S. Chountasis, A. Vourdas, and C. Bendjaballah, Phys. Rev. A. **60**, 3467 (1999).
[33] H. M. Ozaktas, Z. zalevsky, and M. A. Kutay, *The Fractional Fourier Transform: with Applications in Optics and Signal Processing* (John Wiley and Sons Ltd., West Sussex, 2001).
[34] A. W. Lohmann, J. Opt. Soc. Am. A **10**, 2181 (1993).
[35] J. W. Goodman, *Introduction to Fourier Optics* (Mc Graw Hill, Boston, 1996).
[36] C. H. Monken (2002), unpublished lecture notes.
[37] A. N. Oliveira, P. L. Saldanha, and C. H. Monken.
[38] T. B. Pittman, D. V. Strekalov, D. N. Klyshko, M. H. Rubin, A. V. Sergienko, and Y. H. Shih, Phys.Rev. A **53**, 2804 (1996).
[39] G. R. Fowles, *Introduction to Modern Optics* (Dover, New York, 1989).
[40] M. P. Almeida, S. P. Walborn, and P. H. S. Ribeiro, Phys. Rev. A **72**, 022313 (2005).
[41] The relevant parameter here is the FRFT system with the smaller value of $f\Delta\theta/2$, since it is the strictest "filter" of the angle distribution.